

HEXAGONS AND SOLITON-LIKE SPIKES: RADIOSCOPY OF THE ROSENSWEIG INSTABILITY

*R. Richter*¹, *I.V. Barashenkov*², *H. Knieling*¹,
*C. Gollwitzer*¹, *I. Rehberg*¹

¹ *Experimentalphysik V, Univ. Bayreuth, D-95440 Bayreuth, Germany*

² *University of Cape Town, Rondebosch 7700, South Africa*

We report an observation of a stable soliton-like structure on the surface of a ferrofluid, generated by a local perturbation in the hysteretic regime of the Rosensweig instability. Unlike other pattern-forming systems with localized 2D structures, magnetic fluids are characterized by energy conservation; hence, their mechanism of soliton stabilization is different from the previously discussed gain/loss balance mechanism. The radiosopic measurements of the soliton's surface profile suggest that locking on the underlying periodic structure is instrumental in its stabilization.

Introduction. To date, stable solitary waves have been experimentally observed in a variety of one-dimensional and quasi-one-dimensional physical systems. In 2D, dispersive nonlinear systems are prone to collapse instabilities and hence the 2D solitons turned out to be more elusive. (Here we use the term “soliton” in a broad physical sense as a synonym of localized structure.) So far, the list of experimentally detectable 2D localized objects was confined mostly to vortices in superfluids, superconductors, and other media, on one hand, and dissipative solitons in nonequilibrium systems, on the other. While the stability of the former is due to their nontrivial topology, the latter come into being via the balance of strong dissipation and energy gain. Examples include current filaments in gas discharge systems [1]; oscillons in fluids and granular materials [2]; breathing spots in chemical reactions [3] and feedback and cavity solitons in optics [4]. Despite some encouraging theoretical insights, the question of whether 2D non topological solitons can arise in *conservative* systems has remained open.

Here we report an experimental observation of a strongly localized, stable stationary soliton on the surface of magnetic fluid (MF) in a stationary magnetic field. The MF is a dispersion of magnetic nanoparticles, and thus has a high relative permeability μ_r [5]. This is a lossless system; a horizontal layer of the MF in a vertically applied magnetic induction \mathbf{B} is characterized by the energy density [6, 7]:

$$\mathcal{F}(h) = \frac{\rho g}{2} h^2 - \int_0^h dz \mathbf{B} \frac{\mu_r - 1}{2} \mathbf{H}_{\text{MF}}(x, y, z) + \sigma \sqrt{1 + (\partial_x h)^2 + (\partial_y h)^2}. \quad (1)$$

Here ρ and σ are the density and surface tension of the MF, $h(x, y)$ is the local height of the liquid layer, and $\mathbf{H}_{\text{MF}}(x, y, z)$ is the magnetic field in the presence of the MF. The three terms in Eq. (1) represent the hydrostatic, magnetic and surface energy, respectively. As the surface profile deviates from the flat reference state, the first and last term grow, whereas the magnetic energy decreases. For sufficiently large \mathbf{B} , this gives rise to the Rosensweig instability [8, 5].

1. Experimental setup. Our experimental setup is sketched in Fig. 1a. A Teflon[®] vessel with the radius $R = 60$ mm and depth of 3 mm [9] is filled with the MF up to the brim and placed on the common axis midway between two Helmholtz coils. An x-ray tube is mounted above the center. The radiation transmitted through the fluid layer and the bottom of the vessel is recorded by an

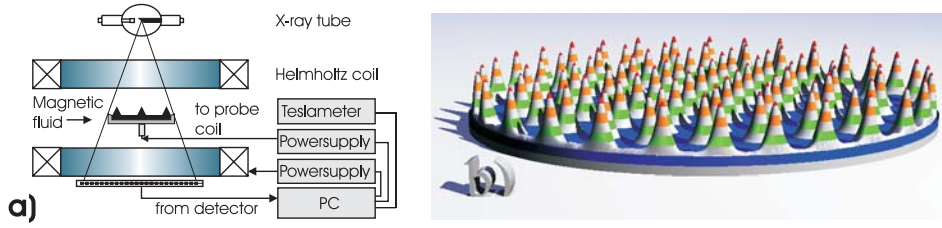


Fig. 1. Radioscopy: (a) sketch of the experimental setup; (b) reconstruction of the surface relief for $B = 10.407$ mT. Each color marks a layer of 1 mm.

x-ray sensitive photodiode array detector (16 bit) connected to a computer. The full surface relief is then reconstructed from the calibrated radioscopic images, as shown in Fig. 1b. For details see [10]. The experiments were performed with the magnetic fluid EMG 901 from Ferrotec. Its material parameters are $\mu_r = 3.2$, $\rho = 1.406$ g cm $^{-3}$, and $\sigma = 25 \pm 0.7$ mN/m.

2. Results. We measured the top-to-bottom height A of the stationary fluid pattern arising in the adiabatic increase and decrease of B . To avoid the edge-induced imperfections in the character of the bifurcation, we only consider spikes located within 11 mm from the center of the dish. Fig. 2 displays results obtained for 400 values of B . As B is increased, a sudden transition to the upper branch occurs at $B_c = 9.025$ mT. For $B > B_c$, the entire surface is covered with a lattice of liquid spikes, which is hexagonal away from the boundary. Decreasing B , the order parameter A remains on the upper branch all the way to $B^* = 8.076$ mT, where it drops to the flat reference level. The subcritical bifurcation to hexagons is described by the amplitude equation $\epsilon A + \gamma(1 + \epsilon)A^2 - gA^3 = 0$ of Ref. [7]. The solid (dashed) lines display the least square fit to the roots

$$A_{\pm} = [\gamma(1 + \epsilon) \pm \sqrt{\gamma^2(1 + \epsilon)^2 + 4\epsilon g}]/(2g), \quad (2)$$

with $\gamma = 0.281$ and $g = 0.062$.

To study the stability of the flat surface to local perturbations (in the hysteric regime), a small air coil with the inner diameter of 8 mm was placed under

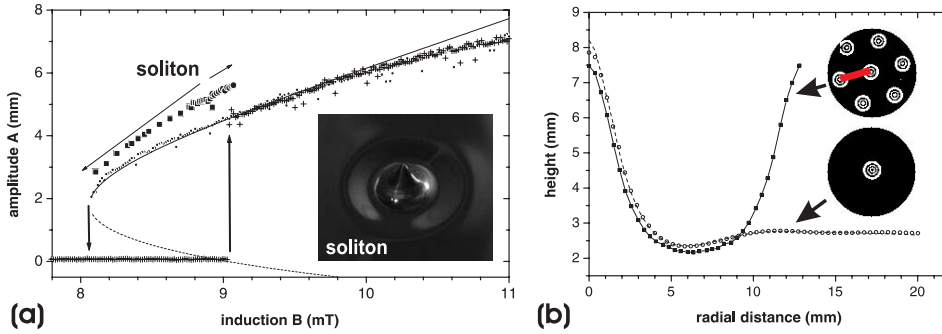


Fig. 2. (a) The amplitude of the pattern for $r < 11$ mm versus the magnetic induction. The crosses (dots) mark the values for increasing (decreasing) induction, respectively. The solid (dashed) lines display the least square fit to Eq. (2). The full circles (squares) give the amplitude of the localized spike initiated at $B = 8.91$ mT for increasing (decreasing) induction, respectively. (b) The filled squares mark the profile of one period of the hexagonal pattern, measured at $B = 9.07$ mT in the center of the vessel; $r < 8.8$ mm. Azimuthally averaged height profiles of two different solitons, measured at the same induction, are depicted by open symbols (one) and a dashed line (the other).

the center of the vessel (see Fig. 1a). This allows to increase, locally, the magnetic induction. A local pulse of $B_+ = 0.68 \text{ mT}$, added to the uniform field of $B = 8.91 \text{ mT}$, produces a single stationary spike of fluid, surrounded by a circular dip, which does not disperse after B_+ has been turned off. The inset of Fig. 1b presents a photo of this radially-symmetric state, which will be referred to as the soliton. The soliton is a stable nondecaying structure; it remained intact for days.

We examined the range of stability of a soliton generated by a pulse with $B_+ = 0.68 \text{ mT}$ added to the uniform induction $B = 8.91 \text{ mT}$. Reducing B adiabatically we measured the corresponding amplitude of the soliton (marked with full squares in Fig. 2a). Similarly to the spikes in the hexagonal pattern, the height of the soliton decreases as B is reduced. The soliton decays for $B < 8.09 \text{ mT}$, which is close to $B^* = 8.076 \text{ mT}$, the lower stability boundary of the hexagonal pattern. As B is increased, the amplitude of the soliton grows, as indicated in Fig. 2a with full circles. At $B = 9.055 \text{ mT}$, a sudden transition from the soliton to a fully developed Rosensweig pattern occurs.

In order to illustrate the robustness of the soliton's shape, we show in Fig. 2b the azimuthally averaged profiles of two different solitons, produced in two separate experiments at $B = 9.07 \text{ mT}$. The profiles are practically indistinguishable. Also plotted are two half-periods of the corresponding hexagonal lattice. In agreement with Fig. 2, the soliton is about 1 mm taller than the spikes of the lattice. This may be attributed to the fact that the spikes emerge simultaneously, and thus have to share the liquid available. However, the width of the soliton is very close to the period of the lattice. Therefore, there is a preferred wavelength in the system, to which the soliton locks and stabilizes. A similar stabilization mechanism was discussed before in the context of wave front locking [12]. See also [13]. We have modelled the soliton's stabilization by a conservative analogue of the Swift–Hohenberg equation [11]. The model exhibits a nonmonotonic dispersion relation like in the case of ferrofluids [8].

Applying, repeatedly, pulses of B_+ and allowing the newly born solitons to drift away from the site of the probe coil, we were able to generate two, three, and more solitons. Fig. 3a presents an example of a 9-soliton configuration, with only one remaining at the center. In this way, it is possible to increase the surface energy of the liquid layer in steps. This is illustrated in Fig. 3b which also shows the surface energy of the Rosensweig pattern as a hysteretic function of B .

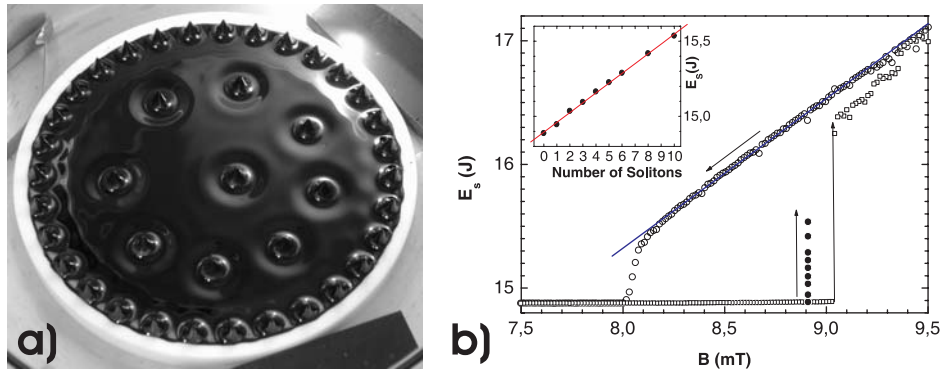


Fig. 3. Multiple Solitons: (a) nine solitons at $B = 8.91 \text{ mT}$. (b) The surface energy of the liquid layer according to Eq. (1) for increasing (open squares) and decreasing (circles) magnetic induction. The full circles mark the increase of E_s through the successive generation of solitons at $B = 8.91 \text{ mT}$ (see inset).

3. Conclusion. We found stable 2D solitons on the surface of a ferrofluid in the hysteretic regime of the Rosensweig instability. These objects are easy to generate and control and they are easily set in motion; this opens ways for studying their binding and scattering. Due to the *conservative nature* of the ferrosolitons, and unlike the localized structures observed previously in dissipative systems, the balance of dissipation and energy gain plays no role in their stabilization. Instead, we suggest a stabilization mechanism which appeals to the locking of the soliton to the wavelength imposed by the nonmonotonic dispersion relation. This mechanism can also be at work in other conservative systems with preferred wavelengths, e.g., in electrostatics and elasticity [14].

Acknowledgements. We thank R. Krauss and C. Lepski for measuring material parameters, and K. Oetter for construction work. Moreover, we are indebted to *Deutsche Forschungsgemeinschaft* for financial support under grant Ri 1054/1-4 and *NRF* of South Africa, for support under grant 205723.

REFERENCES

1. YU.A. ASTROV, YU.A. LOGVIN. *Phys. Rev. Lett.* vol. 79 (1997), p. 2983; I. MÜLLER, E. AMMELT, H.-G. PURWINS, *ibid.* vol. 82 (1999) p. 3428.
2. P.B. UMBANHOWAR, F. MELO, H.L. SWINNEY. *Nature* (London) vol. 382 (1996), p. 793; O. LIOUBASHEVSKI, H. ARBELL, J. FINEBERG. *Phys. Rev. Lett.* vol. 76 (1996), p. 3959; O. LIOUBASHEVSKI *et al.* *ibid.* vol. 83, (1999) p. 3190; H. ARBELL, J. FINEBERG, *ibid.* vol. 85 (2000), p. 756; D. ASTRUC, S. FAUVE. in: *Fluid Mechanics and Its Applications*, vol. 62, pp.39-46 (Kluwer, 2001).
3. D. HAIM *et al.* . *Phys. Rev. Lett.* vol. 77 (1996), p. 190; V.K. VANAG, I.R. EPSTEIN. *ibid.* vol. 92 (2004), p. 128301.
4. V.B. TARANENKO, K. STALIUNAS, C.O. WEISS. *Phys. Rev. A*, vol. 56 (1997), p. 1582; B. SCHÄPERS *et al.* *Phys. Rev. Lett.*, vol. 85 (2000), p. 748; S. BARLAND *et al.* *Nature*, vol. 419 (2002), p. 699.
5. R.E. ROSENSWEIG. *Ferrohydrodynamics* (Cambridge University Press, New York, 1985).
6. A. GAILITIS. *J. Fluid Mech.*, vol. 82 (1977) p. 401.
7. R. FRIEDRICHS, A. ENGEL. *Phys. Rev. E*, vol. 64 (2001), p. 021406.
8. M.D. COWLEY, R.E. ROSENSWEIG. *J. Fluid Mech.*, vol. 30 (1967), p. 671.
9. B. REIMANN, R. RICHTER, I. REHBERG, A. LANGE. *Phys. Rev. E*, vol. 68 (2003), p. 036220.
10. R. RICHTER, J. BLÄSING. *Rev. Sci. Instrum.*, vol. 72 (2001), p. 1729.
11. R. RICHTER, I.V. BARASHENKOV. *Phys. Rev. Lett.*, (2005) (in press).
12. Y. POMEAU. *Physica D*, vol. 23 (1986), p 3.
13. H. SAKAGUCHI, H.R. BRAND. *Europhysics Lett.*, vol. 38 (1997), p 341.
14. G.I. TAYLOR, A.D. MCEWAN. *J. Fluid Mech.*, vol. 22 (1965), p. 1; G.J. STROEBEL, W.H. WARNER *J. Elast.*, vol. 2 (1973), p. 185.